



Research article

Strong Langmuir turbulence dynamics through the trigonometric quintic and exponential B-spline schemes

Mostafa M. A. Khater^{1,2,*} and A. El-Sayed Ahmed³

¹ Department of Mathematics, Faculty of Science, Jiangsu University, 212013, Zhenjiang, China

² Department of Mathematics, Obour High Institute For Engineering and Technology, 11828, Cairo, Egypt

³ Department of Mathematics, Faculty of Science, Taif University P.O. Box 11099, Taif 21944, Saudi Arabia

* **Correspondence:** Email: Mostafa.khater2024@yahoo.com; Tel: +8617851003070, +201149206914.

Abstract: In this manuscript, two recent numerical schemes (the trigonometric quintic and exponential cubic B-spline schemes) are employed for evaluating the approximate solutions of the nonlinear Klein-Gordon-Zakharov model. This model describes the interaction between the Langmuir wave and the ion-acoustic wave in a high-frequency plasma. The initial and boundary conditions are constructed via a novel general computational scheme. [1] has used five different numerical schemes, such as the Adomian decomposition method, Elkalla-expansion method, three-member of the well-known cubic B-spline schemes. Consequently, the comparison between our solutions and that have been given in [1], shows the accuracy of seven recent numerical schemes along with the considered model. The obtained numerical solutions are sketched in two dimensional and column distribution to explain the matching between the computational and numerical simulation. The novelty, originality, and accuracy of this research paper are explained by comparing the obtained numerical solutions with the previously obtained solutions.

Keywords: nonlinear Klein-Gordon-Zakharov (KGZ) model; numerical simulation; the trigonometric quintic (TQBS) and exponential B-spline (ECBS) schemes

Mathematics Subject Classification: 35C07, 76B25, 81Q05, 49M05

1. Introduction

Plasma physics is one of the most attractive branches of science where many scientists have been focusing their attention on discovering more properties of this field [2]. Plasma or cytoplasm is a

distinct state of matter that can be described as an ionized gas in which the electrons are free and are not bound to an atom or a molecule [3]. If the substance is present in nature in three states: solid, liquid, and gas, then plasma can be classified as the fourth state in which the substance can exist [4]. Recently, investigating the heavy Langmuir turbulence's characterization becomes a very important tool for providing a good opportunity to overcome the Langmuir condensation problem [5, 6]. Moreover, this investigation aims to raise the amount of long-wave disturbances through the condensation paradox in Langmuir [7]. At that condensation, the radiation can not dampen the vibration where at severe periods, the coulomb relation is unable to dampen the variations in the pulses because of their frequency [8]. Recently, these radiations with its distinct variations and interactions have been mathematically formulated by some nonlinear evolution equations such as KGZ model [9–12].

The ability of nonlinear partial differential equations with integer or fractional order for formulating different complicated phenomena in various fields including genetics, engineering, quantum mechanics, electro chemistry, chemistry, mechanical engineering, biology, mechanics, etc, makes it the ideal and direct way for discovering the undiscoverable properties of these phenomena [13–19]. Thus, many mathematicians and physics pay complete attention to derive computational, semi-analytical, numerical techniques for solving these equations such as the Adomian decomposition method, Elkalla expansion method, B-spline schemes, extended simplest equation method, modified Khater method, generalized Khater method, exponential expansion method, auxiliary equation method, direct algebraic expansion method, and so no [20–28]. These methods have been employed on several models but until now, there is no unified method can be applied to all the nonlinear evolution equation [29–32].

In this context, this paper investigate the numerical solutions of the nonlinear KGZ model. This model is formulates as follows [33–35]:

$$\begin{cases} \mathcal{G}_{tt} - \mathcal{G}_{xx} + \mathcal{G} + \nu_0 \mathcal{Q}\mathcal{G} = 0, \\ \mathcal{Q}_{tt} - \mathcal{Q}_{xx} - \nu_1 (|\mathcal{G}|^2)_{xx}, \end{cases} \quad (1.1)$$

where ν_0, ν_1 are nonzero real parameters describing the consistency of the initial data of the KGZ system while $\mathcal{Q} = \mathcal{Q}(x, t)$, $\mathcal{G} = \mathcal{G}(x, t)$ are receptively real and complex functions which represent the fast time scale component of the electric field raised by electrons and the derivation of ion density from its equilibrium. Eq (1.1) describes the interaction and contact between the Langmuir wave and the acoustic wave of the ions in a high frequency plasma. [1] have employed the generalized Khater method to Eq (1.1) and converted it into the following ordinary differential equation with the following initial and boundary conditions

$$\begin{cases} \mathfrak{P}'' + \mathcal{L}_1 \mathfrak{P} + \mathcal{L}_2 \mathfrak{P}^3 = 0, \\ \mathfrak{P}(0) = \mathcal{F}(\mathfrak{z}), \mathfrak{P}_3(0) = \mathcal{E}(\mathfrak{z}). \end{cases} \quad (1.2)$$

The generalized Khater method have been constructed the values of \mathcal{F} , \mathcal{E} under the following value of

the above-mentioned parameters $\mathcal{L}_0 = \frac{1}{2}$, $\mathcal{L}_1 = -\frac{225}{32}$ as follows [1]:

$$\begin{cases} \mathcal{F}(3) = \frac{1}{15}(-4) \tanh\left(\frac{3}{2}\right), \\ \mathcal{E}(3) = -\frac{2}{15}. \end{cases} \quad (1.3)$$

This model can be used to calculate from Euler's equations for electrons and ions, with Maxwell's electromagnetic field law for ions, by disregarding the influence of magnetic fields [36, 37]. The nonlinear KGZ model has numerically studied through some recent approximate schemes such as a finite difference method [38] where Chunmei Su and Wenfan Yi have investigated the numerical solutions and established the error estimates of a conservative finite difference method for the considered model with a dimensionless parameter $0 < \varepsilon \ll 1$, which is inversely proportional to the speed of sound. While [39] has compared the obtained numerical solutions that have been obtained through applying Finite difference time domain (FDTD) methods, Exponential wave integrator (EWI) and Time-splitting (TS) method, Uniformly and optimally accurate (UOA) methods and Uniformly accurate (UA) methods that have been applied in [40, 41] of the same model that give a precision, computational sophistication, and other properties are also addressed. [15] has employed the well-known Chebyshev Cardinal Functions for investigating the numerical solutions of the nonlinear KGZ model where operational matrices of derivatives have been used to convert partial differential equations into nonlinear algebraic equations. [16] has used a new conservative finite difference scheme with a parameter θ has been employed for obtaining the numerical solutions of the considered model. Moreover, Convergence of the numerical solutions has been investigated. For further information of the numerical solutions of the nonlinear KGZ model, you can see [17, 18].

The rest sections in this manuscript is organized as follows; Section 2 applies the above-mentioned numerical schemes to the nonlinear KGZ equation for estimating the numerical solutions. Section 3 discusses the obtained numerical solutions. Section 4 gives the conclusion of the whole paper.

2. Numerical investigation

Here, we give the headline of the used methods they we give the obtained results along with these approximate schemes

2.1. Methodology

2.1.1. Trigonometric Quintic B-spline scheme

Using the trigonometric Quintic B-spline scheme supposes the solutions of Eq (1.2) is formulated as following

$$\mathfrak{P}(3) = \sum_{j=-2}^{r+2} C_j \mathcal{G}_j(3), \quad j = (0, 1, \dots, r), \quad (2.1)$$

where C_j are determined from the collocation points z_j and $\mathcal{G}_j(z)$ satisfies the following values

$$\mathcal{G}_j(z) = \begin{cases} \psi^5(z_{j-3}), & z \in [z_{j-3}, z_{j-2}] \\ \psi^4(z_{j-3}) \Psi(z_{j-1}) + \cdots + \Psi(z_{j+3}) \psi^4(z_{j-2}) & z \in [z_{j-2}, z_{j-1}] \\ \psi^3(z_{j-3}) \Psi^2(z_j) + \cdots + \Psi^2(z_{j+3}) \psi^3(z_{j-1}) & z \in [z_{j-1}, z_j] \\ \psi^2(z_{j-3}) \Psi^3(z_{j+1}) + \cdots + \Psi^3(z_{j+3}) \psi^2(z_j) & z \in [z_j, z_{j+1}] \\ \psi(z_{j-1}) \Psi^2(z_{j+2}) + \cdots + \Psi^4(z_{j+3}) \psi(z_{j+1}), & z \in [z_{j+1}, z_{j+2}] \\ \Psi^5(z_{j+3}) & z \in [z_{j+2}, z_{j+3}] \\ 0, & \text{otherwise} \end{cases} \quad (2.2)$$

where $\psi(z_j) = \sin\left(\frac{z_j - z_j}{2}\right)$, $\Psi(z_j) = \sin\left(\frac{z_j - z_j}{2}\right)$. Consequently, we can find the values of $\mathcal{G}_j(z)$ as shown in the next Table 1 where the values of \mathcal{P}_L , $L = 1, \dots, 13$.

Table 1. Value of $\mathcal{G}_j(z)$ and its principle two derivatives at the knot points.

z	z_{j-3}	z_{j-2}	z_{j-1}	z_j	z_{j+1}	z_{j+2}	z_{j+3}
$\mathcal{G}_j(z)$	0	\mathcal{P}_1	\mathcal{P}_2	\mathcal{P}_3	\mathcal{P}_2	\mathcal{P}_1	0
$\mathcal{G}'_j(z)$	0	$-\mathcal{P}_4$	$-\mathcal{P}_5$	0	\mathcal{P}_5	\mathcal{P}_4	0
$\mathcal{G}''_j(z)$	0	\mathcal{P}_6	\mathcal{P}_7	\mathcal{P}_8	\mathcal{P}_7	\mathcal{P}_6	0
$\mathcal{G}'''_j(z)$	0	\mathcal{P}_9	\mathcal{P}_{10}	0	\mathcal{P}_{10}	\mathcal{P}_9	0
$\mathcal{G}''''_j(z)$	0	\mathcal{P}_{11}	\mathcal{P}_{12}	\mathcal{P}_{13}	\mathcal{P}_{12}	\mathcal{P}_{11}	0

$$\mathcal{P}_1 = \frac{\sin^5\left(\frac{h}{2}\right)}{\sin\left(\frac{5h}{2}\right) \sin(2h) \sin\left(\frac{3h}{2}\right) \sin(h) \sin\left(\frac{h}{2}\right)}, \quad (2.3)$$

$$\mathcal{P}_2 = \frac{2 \sin^5\left(\frac{h}{2}\right) \cos\left(\frac{h}{2}\right) \left(16 \cos^2\left(\frac{h}{2}\right) - 3\right)}{\sin\left(\frac{5h}{2}\right) \sin(2h) \sin\left(\frac{3h}{2}\right) \sin(h) \sin\left(\frac{h}{2}\right)}, \quad (2.4)$$

$$\mathcal{P}_3 = \frac{2 \sin^5\left(\frac{h}{2}\right) \left(48 \cos^4\left(\frac{h}{2}\right) - 16 \cos^2\left(\frac{h}{2}\right) + 1\right)}{\sin\left(\frac{5h}{2}\right) \sin(2h) \sin\left(\frac{3h}{2}\right) \sin(h) \sin\left(\frac{h}{2}\right)}, \quad (2.5)$$

$$\mathcal{P}_4 = \frac{5 \sin^4\left(\frac{h}{2}\right) \cos\left(\frac{h}{2}\right)}{2 \left(\sin\left(\frac{5h}{2}\right) \sin(2h) \sin\left(\frac{3h}{2}\right) \sin(h) \sin\left(\frac{h}{2}\right)\right)}, \quad (2.6)$$

$$\mathcal{P}_5 = \frac{5 \sin^4\left(\frac{h}{2}\right) \cos^2\left(\frac{h}{2}\right) \left(8 \cos^2\left(\frac{h}{2}\right) - 3\right)}{\sin\left(\frac{5h}{2}\right) \sin(2h) \sin\left(\frac{3h}{2}\right) \sin(h) \sin\left(\frac{h}{2}\right)}, \quad (2.7)$$

$$\mathcal{P}_6 = \frac{5 \sin^3\left(\frac{h}{2}\right) \left(5 \cos^2\left(\frac{h}{2}\right) - 1\right)}{4 \left(\sin\left(\frac{5h}{2}\right) \sin(2h) \sin\left(\frac{3h}{2}\right) \sin(h) \sin\left(\frac{h}{2}\right)\right)}, \quad (2.8)$$

$$\mathcal{P}_7 = \frac{5 \sin^3\left(\frac{h}{2}\right) \cos\left(\frac{h}{2}\right) \left(16 \cos^4\left(\frac{h}{2}\right) - 15 \cos^2\left(\frac{h}{2}\right) + 3\right)}{2 \left(\sin\left(\frac{5h}{2}\right) \sin(2h) \sin\left(\frac{3h}{2}\right) \sin(h) \sin\left(\frac{h}{2}\right)\right)}, \quad (2.9)$$

$$\mathcal{P}_8 = -\frac{5 \sin^3\left(\frac{h}{2}\right) \left(16 \cos^6\left(\frac{h}{2}\right) - 5 \cos^2\left(\frac{h}{2}\right) + 1\right)}{2 \left(\sin\left(\frac{5h}{2}\right) \sin(2h) \sin\left(\frac{3h}{2}\right) \sin(h) \sin\left(\frac{h}{2}\right)\right)}, \quad (2.10)$$

$$\mathcal{P}_9 = \frac{5 \sin^2\left(\frac{h}{2}\right) \cos\left(\frac{h}{2}\right) (25 \cos(h) - 1)}{16 \left(\sin\left(\frac{5h}{2}\right) \sin(2h) \sin\left(\frac{3h}{2}\right) \sin(h) \sin\left(\frac{h}{2}\right)\right)}, \quad (2.11)$$

$$\mathcal{P}_{10} = -\frac{5 \sin^2(h) (-27 \cos(h) + 2 \cos(2h) + 1)}{32 \left(\sin\left(\frac{5h}{2}\right) \sin(2h) \sin\left(\frac{3h}{2}\right) \sin(h) \sin\left(\frac{h}{2}\right)\right)}, \quad (2.12)$$

$$\mathcal{P}_{11} = \frac{5 \sin\left(\frac{h}{2}\right) (44 \cos(h) + 125 \cos(2h) + 23)}{128 \left(\sin\left(\frac{5h}{2}\right) \sin(2h) \sin\left(\frac{3h}{2}\right) \sin(h) \sin\left(\frac{h}{2}\right)\right)}, \quad (2.13)$$

$$\mathcal{P}_{12} = -\frac{5 \sin(h) (88 \cos(h) + 127 \cos(2h) + 44 \cos(3h) + 125)}{128 \left(\sin\left(\frac{5h}{2}\right) \sin(2h) \sin\left(\frac{3h}{2}\right) \sin(h) \sin\left(\frac{h}{2}\right)\right)}, \quad (2.14)$$

$$\mathcal{P}_{13} = \frac{5 \sin\left(\frac{h}{2}\right) (2 \cos(h) + 1) (125 \cos(h) + 21 \cos(2h) + 23 \cos(3h) + 23)}{64 \left(\sin\left(\frac{5h}{2}\right) \sin(2h) \sin\left(\frac{3h}{2}\right) \sin(h) \sin\left(\frac{h}{2}\right)\right)}, \quad (2.15)$$

where $h = \frac{q-p}{r}$, $q > p$ such that $[p, q]$ is the problem's domain.

2.1.2. Exponential cubic B-spline schemes

Employing the exponential cubic spline technique to considered model with the above conditions, yields elicit its numerical solutions as following

$$\mathfrak{P}(3) = \sum_{\mathfrak{x}=-1}^{\mathfrak{M}+1} \mathfrak{C}_{\mathfrak{x}} \mathcal{E}_{\mathfrak{x}}, \quad (2.16)$$

where $\mathfrak{C}_{\mathfrak{I}}$, $\mathfrak{E}_{\mathfrak{I}}$ follow the next conditions, respectively:

$$\mathfrak{L} \mathfrak{B}(\mathfrak{z}) = \mathcal{F}(\mathfrak{z}_{\mathfrak{I}}, \mathfrak{B}(\mathfrak{z}_{\mathfrak{I}})) \text{ where } (\mathfrak{I} = 0, 1, \dots, n)$$

and

$$\mathfrak{E}_{\mathfrak{I}}(\mathfrak{z}) = \frac{1}{6 \mathfrak{H}^3} \begin{cases} (\mathfrak{z} - \mathfrak{z}_{\mathfrak{I}-2})^3, & \mathfrak{z} \in [\mathfrak{z}_{\mathfrak{I}-2}, \mathfrak{z}_{\mathfrak{I}-1}], \\ -3(\mathfrak{z} - \mathfrak{z}_{\mathfrak{I}-1})^3 + 3 \mathfrak{H}(\mathfrak{z} - \mathfrak{z}_{\mathfrak{I}-1})^2 + 3 \mathfrak{H}^2(\mathfrak{z} - \mathfrak{z}_{\mathfrak{I}-1}) + \mathfrak{H}^3, & \mathfrak{z} \in [\mathfrak{z}_{\mathfrak{I}-1}, \mathfrak{z}_{\mathfrak{I}}], \\ -3(\mathfrak{z}_{\mathfrak{I}+1} - \mathfrak{z})^3 + 3 \mathfrak{H}(\mathfrak{z}_{\mathfrak{I}+1} - \mathfrak{z})^2 + 3 \mathfrak{H}^2(\mathfrak{z}_{\mathfrak{I}+1} - \mathfrak{z}) + \mathfrak{H}^3, & \mathfrak{z} \in [\mathfrak{z}_{\mathfrak{I}}, \mathfrak{z}_{\mathfrak{I}+1}], \\ (\mathfrak{z}_{\mathfrak{I}+2} - \mathfrak{z})^3, & \mathfrak{z} \in [\mathfrak{z}_{\mathfrak{I}+1}, \mathfrak{z}_{\mathfrak{I}+2}], \\ 0, & \text{otherwise.} \end{cases} \quad (2.17)$$

For $\mathfrak{I} \in [-2, \mathfrak{M} + 2]$, we obtain

$$\mathfrak{B}_{\mathfrak{I}}(\mathfrak{z}) = \mathfrak{C}_{\mathfrak{I}-1} + 4 \mathfrak{C}_{\mathfrak{I}} + \mathfrak{C}_{\mathfrak{I}+1}. \quad (2.18)$$

2.2. Method's results

Here, we apply the TQBS and ECBS schemes to Eq (1.1) with the evaluated initial and boundary conditions (1.3) as following.

2.2.1. Numerical solution via TQBS scheme

Applying the TQBS scheme to Eq (1.2) with above-conditions (1.3), gets the following numerical values in Tables 2, 3, and Figure 1.

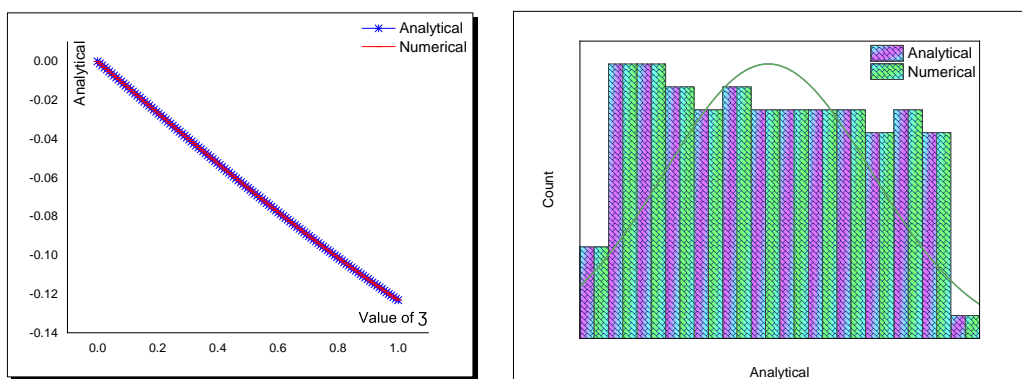


Figure 1. analytical, numerical, and absolute error for the nonlinear KGZ equations through the TQBS scheme.

Table 2. Analytical, numerical, and absolute error of Eq (1.2) through the TQBS scheme under the shown values of boundary and initial conditions (1.3).

Value of β	Analytical	Numerical	Absolute Error	Value of β	Analytical	Numerical	Absolute Error
0	0	-2.71051E-20	2.71051E-20	0.2578125	-0.034185856	-0.034185856	4.37705E-14
0.0078125	-0.001041661	-0.001041661	1.00159E-15	0.265625	-0.035209885	-0.035209885	4.49224E-14
0.015625	-0.002083291	-0.002083291	2.52879E-15	0.2734375	-0.036232859	-0.036232859	4.60743E-14
0.0234375	-0.003124857	-0.003124857	3.91484E-15	0.28125	-0.037254747	-0.037254747	4.72261E-14
0.03125	-0.004166328	-0.004166328	5.33774E-15	0.2890625	-0.038275521	-0.038275521	4.83363E-14
0.0390625	-0.005207671	-0.005207671	6.74634E-15	0.296875	-0.039295151	-0.039295151	4.94466E-14
0.046875	-0.006248856	-0.006248856	8.1584E-15	0.3046875	-0.040313607	-0.040313607	5.05221E-14
0.0546875	-0.00728985	-0.00728985	9.56613E-15	0.3125	-0.041330861	-0.041330861	5.15907E-14
0.0625	-0.008330622	-0.008330622	1.09721E-14	0.3203125	-0.042346885	-0.042346885	5.26246E-14
0.0703125	-0.00937114	-0.00937114	1.23738E-14	0.328125	-0.043361648	-0.043361648	5.36515E-14
0.078125	-0.010411372	-0.010411372	1.37685E-14	0.3359375	-0.044375124	-0.044375124	5.46438E-14
0.0859375	-0.011451287	-0.011451287	1.51632E-14	0.34375	-0.045387282	-0.045387282	5.56291E-14
0.09375	-0.012490853	-0.012490853	1.65527E-14	0.3515625	-0.046398096	-0.046398096	5.65936E-14
0.1015625	-0.013530039	-0.013530039	1.7937E-14	0.359375	-0.047407536	-0.047407536	5.75304E-14
0.109375	-0.014568812	-0.014568812	1.93196E-14	0.3671875	-0.048415576	-0.048415576	5.84324E-14
0.1171875	-0.015607143	-0.015607143	2.06935E-14	0.375	-0.049422187	-0.049422187	5.93275E-14
0.125	-0.016644999	-0.016644999	2.20587E-14	0.3828125	-0.050427341	-0.050427341	6.02018E-14
0.1328125	-0.017682349	-0.017682349	2.34222E-14	0.390625	-0.051431011	-0.051431011	6.10553E-14
0.140625	-0.018719162	-0.018719162	2.47719E-14	0.3984375	-0.052433171	-0.052433171	6.1888E-14
0.1484375	-0.019755406	-0.019755406	2.6118E-14	0.40625	-0.053433792	-0.053433792	6.2686E-14
0.15625	-0.020791051	-0.020791051	2.74503E-14	0.4140625	-0.054432847	-0.054432847	6.34492E-14
0.1640625	-0.021826065	-0.021826065	2.87825E-14	0.421875	-0.055430311	-0.055430311	6.41917E-14
0.171875	-0.022860418	-0.022860418	3.01044E-14	0.4296875	-0.056426157	-0.056426157	6.48925E-14
0.1796875	-0.023894078	-0.023894078	3.14124E-14	0.4375	-0.057420357	-0.057420357	6.56003E-14
0.1875	-0.024927014	-0.024927014	3.26926E-14	0.4453125	-0.058412887	-0.058412887	6.62456E-14
0.1953125	-0.025959197	-0.025959197	3.39763E-14	0.453125	-0.059403719	-0.059403719	6.68632E-14
0.203125	-0.026990595	-0.026990595	3.52322E-14	0.4609375	-0.060392829	-0.060392829	6.74669E-14
0.2109375	-0.028021178	-0.028021178	3.64916E-14	0.46875	-0.06138019	-0.06138019	6.80359E-14
0.21875	-0.029050915	-0.029050915	3.77406E-14	0.4765625	-0.062365777	-0.062365777	6.8591E-14
0.2265625	-0.030079776	-0.030079776	3.89688E-14	0.484375	-0.063349565	-0.063349565	6.91253E-14
0.234375	-0.03110773	-0.03110773	4.01866E-14	0.4921875	-0.064331528	-0.064331528	6.95971E-14
0.2421875	-0.032134749	-0.032134749	4.13905E-14	0.5	-0.065311643	-0.065311643	7.00412E-14
0.25	-0.0331608	-0.0331608	4.25909E-14	0.5078125	-0.066289885	-0.066289885	7.04575E-14

Table 3. Analytical, numerical, and absolute error of Eq (1.2) through the TQBS scheme under the shown values of boundary and initial conditions (1.3).

Value of β	Analytical	Numerical	Absolute error	Value of β	Analytical	Numerical	Absolute error
0.515625	-0.067266228	-0.067266228	7.08461E-14	0.7578125	-0.096468595	-0.096468595	6.22696E-14
0.5234375	-0.068240649	-0.068240649	7.11931E-14	0.765625	-0.097372658	-0.097372658	6.1201E-14
e 0.53125	-0.069213124	-0.069213124	7.14984E-14	0.7734375	-0.098274146	-0.098274146	6.00908E-14
0.5390625	-0.070183629	-0.070183629	7.18037E-14	0.78125	-0.099173043	-0.099173043	5.88973E-14
0.546875	-0.071152141	-0.071152141	7.20674E-14	0.7890625	-0.100069331	-0.100069331	5.76483E-14
0.5546875	-0.072118635	-0.072118635	7.22755E-14	0.796875	-0.100962996	-0.100962996	5.63855E-14
0.5625	-0.07308309	-0.07308309	7.24559E-14	0.8046875	-0.101854021	-0.101854021	5.50393E-14
0.5703125	-0.074045483	-0.074045483	7.25808E-14	0.8125	-0.102742391	-0.102742391	5.36515E-14
0.578125	-0.075005789	-0.075005789	7.2678E-14	0.8203125	-0.103628091	-0.103628091	5.21666E-14
0.5859375	-0.075963988	-0.075963988	7.27196E-14	0.828125	-0.104511107	-0.104511107	5.06262E-14
0.59375	-0.076920057	-0.076920057	7.27474E-14	0.8359375	-0.105391423	-0.105391423	4.89747E-14
0.6015625	-0.077873973	-0.077873973	7.27057E-14	0.84375	-0.106269025	-0.106269025	4.72677E-14
0.609375	-0.078825716	-0.078825716	7.26502E-14	0.8515625	-0.107143899	-0.107143899	4.55053E-14
0.6171875	-0.079775264	-0.079775264	7.25253E-14	0.859375	-0.108016031	-0.108016031	4.36595E-14
0.625	-0.080722594	-0.080722594	7.23588E-14	0.8671875	-0.108885407	-0.108885407	4.17999E-14
0.6328125	-0.081667688	-0.081667688	7.21367E-14	0.875	-0.109752015	-0.109752015	3.98431E-14
0.640625	-0.082610522	-0.082610522	7.18869E-14	0.8828125	-0.110615841	-0.110615841	3.78308E-14
0.6484375	-0.083551078	-0.083551078	7.15816E-14	0.890625	-0.111476871	-0.111476871	3.57908E-14
0.65625	-0.084489334	-0.084489334	7.12486E-14	0.8984375	-0.112335095	-0.112335095	3.36675E-14
0.6640625	-0.08542527	-0.08542527	7.086E-14	0.90625	-0.113190498	-0.113190498	3.14748E-14
0.671875	-0.086358867	-0.086358867	7.04575E-14	0.9140625	-0.11404307	-0.11404307	2.92405E-14
0.6796875	-0.087290105	-0.087290105	6.99718E-14	0.921875	-0.114892798	-0.114892798	2.68674E-14
0.6875	-0.088218965	-0.088218965	6.94583E-14	0.9296875	-0.11573967	-0.11573967	2.44249E-14
0.6953125	-0.089145427	-0.089145427	6.88755E-14	0.9375	-0.116583676	-0.116583676	2.18991E-14
0.703125	-0.090069472	-0.090069472	6.82371E-14	0.9453125	-0.117424804	-0.117424804	1.92901E-14
0.7109375	-0.090991083	-0.090991083	6.75571E-14	0.953125	-0.118263043	-0.118263043	1.66117E-14
0.71875	-0.09191024	-0.09191024	6.68215E-14	0.9609375	-0.119098383	-0.119098383	1.38639E-14
0.7265625	-0.092826925	-0.092826925	6.60166E-14	0.96875	-0.119930814	-0.119930814	1.10745E-14
0.734375	-0.093741121	-0.093741121	6.51562E-14	0.9765625	-0.120760325	-0.120760325	8.18789E-15
0.7421875	-0.094652809	-0.094652809	6.42403E-14	0.984375	-0.121586906	-0.121586906	5.31519E-15
0.75	-0.095561973	-0.095561973	6.32688E-14	0.9921875	-0.122410548	-0.122410548	2.13718E-15

2.2.2. Numerical solution via ECBS scheme

Applying the ECBS scheme to Eq (1.2) with above-conditions (1.3), gets the following numerical values in Table 4, and Figure 2.

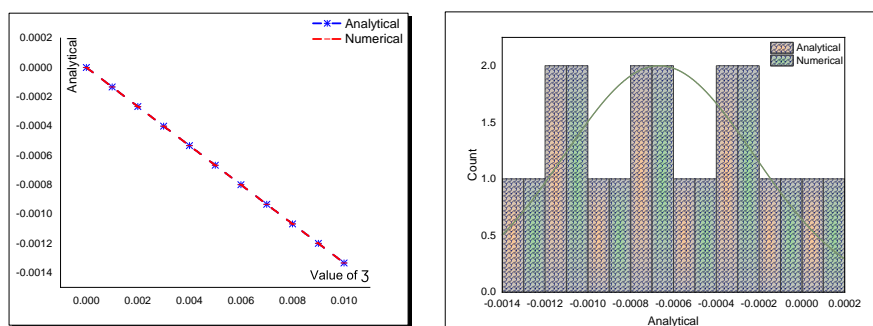


Figure 2. Exact, approximate, and absolute error of the nonlinear KGZ equations through the ECBS scheme.

Table 4. Analytical, numerical, and absolute error of Eq (1.2) through the ECBS scheme under the shown values of boundary and initial conditions (1.3).

Value of β	Analytical	Numerical	Absolute error
0	0	0	0
0.001	-0.000133333	-0.000133333	2.75062E-16
0.002	-0.000266667	-0.000266667	5.33482E-16
0.003	-0.0004	-0.0004	7.58508E-16
0.004	-0.000533333	-0.000533333	9.33498E-16
0.005	-0.000666665	-0.000666665	1.04181E-15
0.006	-0.000799998	-0.000799998	1.06685E-15
0.007	-0.00093333	-0.00093333	9.9172E-16
0.008	-0.001066661	-0.001066661	7.99924E-16
0.009	-0.001199992	-0.001199992	4.75097E-16
0.01	-0.001333322	-0.001333322	0

3. Results and discussion

Here, we explain the accuracy and novelty of the obtained numerical result in this research paper by comparing them with the previously calculated in [42] through four-different schemes (Adomian decomposition (AD), El-kalla (EK), cubic B-spline (CB), and extended cubic B-spline (ECB) schemes)) and one common scheme (exponential cubic B-spline (ExCB) scheme). Although, comparing our obtained result with each other, shows the accuracy of the ECBS scheme over the TQBS scheme where the absolute error is smaller than that have been obtained by the TQBS scheme which have been shown in Figures 1, 2 and Tables 2–4. Now, comparing the accuracy between our solutions and that have been evaluated in [42], shows our solution is more accurate than their solutions that have been explained in Table 5, and Figure 3.

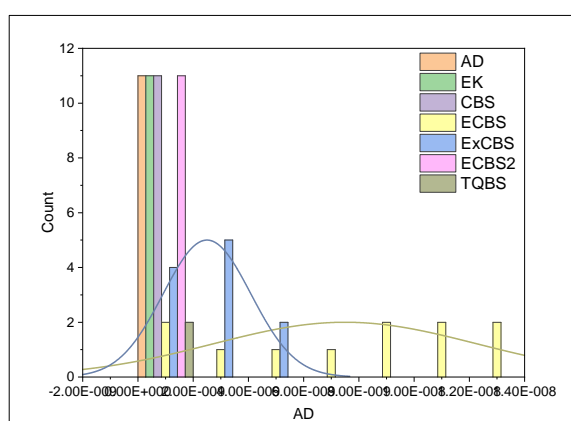


Figure 3. Absolute value of error for AD, EK, CBS, ECBS, ExCBS, ECBS, and TQBS schemes.

Table 5. Numerical methods' absolute error.

Value of β	AD	EK	CBS	EtCBS	ECBS	ECBS	TQBS
0	0	0	0	0	5.45828E-18	0	2.71E-20
0.001	2.71051E-20	2.71051E-20	1.83257E-16	3.29993E-09	1.10002E-09	2.75E-16	
0.002	5.42101E-20	5.42101E-20	3.55401E-16	6.39986E-09	2.13337E-09	5.33E-16	
0.003	0	0	5.05455E-16	9.0998E-09	3.03339E-09	7.59E-16	
0.004	0	0	6.22007E-16	1.11997E-08	3.7334E-09	9.33E-16	
0.005	0	0	6.94215E-16	1.24997E-08	4.16674E-09	1.04E-15	
0.006	1.0842E-19	1.0842E-19	7.10695E-16	1.27997E-08	4.26674E-09	1.07E-15	
0.007	1.0842E-19	1.0842E-19	6.60821E-16	1.18997E-08	3.96674E-09	9.92E-16	
0.008	0	0	5.32994E-16	9.59976E-09	3.20006E-09	8E-16	
0.009	2.1684E-19	0	3.1637E-16	5.69985E-09	1.90003E-09	4.75E-16	
0.01	0	2.1684E-19	0	0	2.1684E-19	0	2.53E-15

4. Conclusions

This manuscript has employed the TQBS and ECBS numerical schemes for evaluating the numerical solutions of the nonlinear KGZ model. The matching between analytical and numerical solutions has been explained through the shown tables and figures. The accuracy of the modified Khater method has been proved through six numerical schemes. The novelty and originality of our obtained solutions have been explained. the powerful and effectiveness of the used techniques are also explained and verified.

Acknowledgments

The authors would like to thank Taif University Researchers supporting Project number (TURSP-2020/159), Taif University-Saudi Arabia.

Conflict of interest

There is no conflict of interest.

References

1. M. M. Khater, D. Lu, On the dynamics of strong Langmuir turbulence through the generalized khater method in the plasma physics, *Eur. Phys. J. Plus*, 2021. Accepted.
2. M. M. Khater, M. Inc, K. Nisar, R. A. Attia, Multi-solitons, lumps, and breath solutions of the water wave propagation with surface tension via four recent computational schemes, *Ain Shams Eng. J.*, 2021. In Press.
3. M. M. Khater, T. A. Nofal, H. Abu-Zinadah, M. S. Lotayif, D. Lu, Novel computational and accurate numerical solutions of the modified Benjamin-Bona-Mahony (BBM) equation arising in the optical illusions field, *Alex. Eng. J.* **60** (2021), 1797–1806.

4. M. M. Khater, M. S. Mohamed, R. A. Attia, On semi analytical and numerical simulations for a mathematical biological model; the time-fractional nonlinear Kolmogorov-Petrovskii-Piskunov (KPP) equation, *Chaos, Solitons Fract.*, **144** (2021), 110676.
5. M. M. Khater, A. Mousa, M. El-Shorbagy, R. A. Attia, Analytical and semi-analytical solutions for Phi-four equation through three recent schemes, *Results Phys.*, **22** (2021), 103954.
6. M. M. Khater, A. E. S. Ahmed, M. El-Shorbagy, Abundant stable computational solutions of Atangana-Baleanu fractional nonlinear HIV-1 infection of CD4⁺ T-cells of immunodeficiency syndrome, *Results Phys.*, **22** (2021), 103890.
7. M. M. Khater, S. Anwar, K. U. Tariq, M. S. Mohamed, Some optical soliton solutions to the perturbed nonlinear Schrödinger equation by modified Khater method, *AIP Adv.*, **11** (2021), 025130.
8. M. M. Khater, R. A. Attia, A. Bekir, D. Lu, Optical soliton structure of the sub-10-fs-pulse propagation model, *J. Optics*, **50** (2021), 109–119.
9. X. Zheng, Y. Shang, X. Peng, Orbital stability of solitary waves of the coupled Klein-Gordon-Zakharov equations, *Math. Method. Appl. Sci.*, **40** (2017), 2623–2633.
10. H. Baskonus, T. Sulaiman, H. Bulut, On the new wave behavior to the Klein-Gordon-Zakharov equations in plasma physics, *Indian J. Phys.*, **93** (2019), 393–399.
11. A. Houwe, S. Abbagari, Y. Salathiel, M. Inc, S. Y. Doka, K. T. Crépin, et al., Complex traveling-wave and solitons solutions to the Klein-Gordon-Zakharov equations, *Results Phys.*, **17** (2020), 103127.
12. S. Nestor, A. Houwe, H. Rezazadeh, A. Bekir, G. Betchewe, S. Y. Doka, New solitary waves for the Klein-Gordon-Zakharov equations, *Mod. Phys. Lett. B*, **34** (2020), 2050246.
13. S. Ali, M. Younis, M. O. Ahmad, S. T. R. Rizvi, Rogue wave solutions in nonlinear optics with coupled Schrödinger equations, *Opt. Quantum Electron.*, **50** (2018), 266.
14. S. T. R. Rizvi, K. Ali, M. Ahmad, Optical solitons for Biswas-Milovic equation by new extended auxiliary equation method, *Optik*, **204** (2020), 164181.
15. I. Ali, S. T. R. Rizvi, S. O. Abbas, Q. Zhou, Optical solitons for modulated compressional dispersive alfvén and heisenberg ferromagnetic spin chains, *Results Phys.*, **15** (2019), 102714.
16. S. R. Rizvi, I. Afzal, K. Ali, M. Younis, Stationary solutions for nonlinear Schrödinger equations by Lie group Analysis, *Acta Phys. Pol. A*, **136** (2019), 187–189.
17. B. Nawaz, K. Ali, S. O. Abbas, S. T. R. Rizvi, Q. Zhou, Optical solitons for non-kerr law nonlinear Schrödinger equation with third and fourth order dispersions, *Chin. J. Phys.*, **60** (2019), 133–140.
18. S. T. R. Rizvi, K. Ali, H. Hanif, Optical solitons in dual core fibers under various nonlinearities, *Mod. Phys. Lett. B*, **33** (2019), 1950189.
19. A. Arif, M. Younis, M. Imran, M. Tantawy, S. T. R. Rizvi, Solitons and lump wave solutions to the graphene thermophoretic motion system with a variable heat transmission, *Eur. Phys. J. Plus*, **134** (2019), 303.
20. P. P. Sullivan, J. C. McWilliams, Langmuir turbulence and filament frontogenesis in the oceanic surface boundary layer, *J. Fluid Mech.*, **879** (2019), 512–553.

21. S. Kim, P. H. Yoon, G. Choe, Y. J. moon, Suprathermal solar wind electrons and Langmuir turbulence, *Astrophys. J.*, **828** (2016), 60.
22. B. G. Reichl, I. Ginis, T. Hara, B. Thomas, T. Kukulka, D. Wang, Impact of sea-state-dependent Langmuir turbulence on the ocean response to a tropical cyclone, *Mon. Weather Rev.*, **144** (2016), 4569–4590.
23. D. Wang, T. Kukulka, B. G. Reichl, T. Hara, I. Ginis, Wind-wave misalignment effects on Langmuir turbulence in tropical cyclone conditions, *J. Phys. Oceanogr.*, **49** (2019), 3109–3126.
24. P. Yoon, M. Lazar, K. Scherer, H. Fichtner, R. Schlickeiser, Modified κ -distribution of solar wind electrons and steady-state Langmuir turbulence, *Astrophys. J.*, **868** (2018), 131.
25. M. Osman, D. Lu, M. M. Khater, A study of optical wave propagation in the nonautonomous schrödinger-hirota equation with power-law nonlinearity, *Results Phys.*, **13** (2019), 102157.
26. M. M. Khater, D. Lu, R. A. Attia, Dispersive long wave of nonlinear fractional Wu-Zhang system via a modified auxiliary equation method, *AIP Adv.*, **9** (2019), 025003.
27. M. M. Khater, D. Lu, R. A. Attia, Erratum: “Dispersive long wave of nonlinear fractional Wu-Zhang system via a modified auxiliary equation method” [AIP adv. 9, 025003 (2019)], *AIP Adv.*, **9** (2019), 049902.
28. M. M. Khater, D. Lu, R. A. Attia, Lump soliton wave solutions for the (2+1)-dimensional Konopelchenko-Dubrovsky equation and KdV equation, *Mod. Phys. Lett. B*, **33** (2019), 1950199.
29. Y. Chu, M. M. Khater, Y. Hamed, Diverse novel analytical and semi-analytical wave solutions of the generalized (2+1)-dimensional shallow water waves model, *AIP Adv.*, **11** (2021), 015223.
30. M. M. Khater, A. Bekir, D. Lu, R. A. Attia, Analytical and semi-analytical solutions for time-fractional Cahn-Allen equation, *Math. Method. Appl. Sci.*, **44** (2021), 2682–2691.
31. E. H. Zahran, M. M. Khater, Modified extended tanh-function method and its applications to the Bogoyavlenskii equation, *Appl. Math. Model.*, **40** (2016), 1769–1775.
32. D. Lu, A. R. Seadawy, M. M. Khater, Structures of exact and solitary optical solutions for the higher-order nonlinear schrödinger equation and its applications in mono-mode optical fibers, *Mod. Phys. Lett. B*, **33** (2019), 1950279.
33. A. Houwe, S. Abbagari, Y. Salathiel, M. Inc, S. Y. Doka, K. T. Crépin, et al., Complex traveling-wave and solitons solutions to the Klein-Gordon-Zakharov equations, *Results Phys.*, **17** (2020), 103127.
34. S. Nestor, A. Houwe, H. Rezazadeh, A. Bekir, G. Betchewe, S. Y. Doka, New solitary waves for the Klein-Gordon-Zakharov equations, *Mod. Phys. Lett. B*, **34** (2020), 2050246.
35. R. Martínez, J. Macías-Díaz, A. Hendy, Corrigendum to a numerically efficient and conservative model for a riesz space-fractional Klein-Gordon-Zakharov system, *Commun. Nonlinear Sci. Numer. Simul.*, **83** (2020), 105109.
36. V. E. Zakharov, Collapse of langmuir waves, *Sov. Phys. JETP*, **35** (1972), 908–914.
37. L. Bergé, B. Bidégaray, T. Colin, A perturbative analysis of the time-envelope approximation in strong langmuir turbulence, *Phys. D: Nonlinear Phenom.*, **95** (1996), 351–379.

38. C. Su, W. Yi, Error estimates of a finite difference method for the Klein-Gordon-Zakharov system in the subsonic limit regime, *IMA J. Numer. Anal.*, **38** (2018), 2055–2073.
39. W. Bao, X. Zhao, Comparison of numerical methods for the nonlinear Klein-Gordon equation in the nonrelativistic limit regime, *J. Comput. Phys.*, **398** (2019), 108886.
40. W. Bao, X. Dong, Analysis and comparison of numerical methods for the Klein-Gordon equation in the nonrelativistic limit regime, *Numer. Math.*, **120** (2012), 189–229.
41. E. Faou, K. Schratz, Asymptotic preserving schemes for the Klein-Gordon equation in the non-relativistic limit regime, *Numer. Math.*, **126** (2014), 441–469.
42. M. M. A. Khater, On the dynamics of strong Langmuir turbulence through the five recent numerical schemes in the plasma physics, *Numer. Method. Part. Differ. Equations*, 2020. Available from: <https://onlinelibrary.wiley.com/doi/abs/10.1002/num.22681>.



AIMS Press

©2021 the Author(s), licensee AIMS Press. This is an open access article distributed under the terms of the Creative Commons Attribution License (<http://creativecommons.org/licenses/by/4.0>)